Journal of Macromolecular Science, Part A
Publication details, including instructions for authors and subscription information:
http://www.informaworld.com/smpp/title~content=t713597274

APPLICATION OF POLYANION/Fe^3 MULTILAYERED MEMBRANES IN PREVENTION OF BIOSENSOR MINERALIZATION

Izabela Galeska[a]; Debjit Chattopadhyay[a]; Fotios Papadimitrakopoulos[a]
[a] Nanomaterials Optoelectronic Laboratory, Department of Chemistry, Institute of Materials Science, University of Connecticut, Storrs, CT, U.S.A.

To cite this Article Galeska, Izabela , Chattopadhyay, Debjit and Papadimitrakopoulos, Fotios(2002) 'APPLICATION OF POLYANION/Fe^3 MULTILAYERED MEMBRANES IN PREVENTION OF BIOSENSOR MINERALIZATION', Journal of Macromolecular Science, Part A, 39: 10, 1207 — 1222

To link to this Article: DOI: 10.1081/MA-120014846

URL: http://dx.doi.org/10.1081/MA-120014846

MARCEL DEKKER, INC. • 270 MADISON AVENUE • NEW YORK, NY 10016

JOURNAL OF MACROMOLECULAR SCIENCE
Part A—Pure and Applied Chemistry
Vol. A39, No. 10, pp. 1207–1222, 2002

APPLICATION OF POLYANION/Fe^{3+} MULTILAYERED MEMBRANES IN PREVENTION OF BIOSENSOR MINERALIZATION

Izabela Galeska, Debjit Chattopadhyay, and Fotios Papadimitrakopoulos*

Nanomaterials Optoelectronic Laboratory, Department of
Chemistry, Polymer Program, Institute of Materials Science,
University of Connecticut, Storrs, CT 06269

ABSTRACT

Controlled analyte permeability, calcification resistance and biocompatibility are among the many prerequisites necessary for the fabrication of outer membranes for implantable biosensors. In this study, multilayered films of polyelectrolytes (i.e., Nafion^{TM}, a perfluorinated ionomer, and Humic Acids (HAs), naturally occurring biopolymers) were investigated as potential semi-permeable membranes for implantable glucose sensors. These films were fabricated using the layer-by-layer self-assembly of polyanions (either Nafion or HAs) with oppositely charged ferric ions. Spectroscopic and quartz crystal microbalance (QCM) studies point towards a stepwise film growth pattern, with growth rates as high as 47 and 24.3 nm per layer for Nafion and HAs, respectively. These assemblies were characterized by growth rates that are strongly dependent on the pH and ionic strength of the polyanion solution. Nafion/Fe^{3+} assembled films exhibit an order of magnitude lower calcification level as compared to dip-coated and annealed Nafion films. Additionally, these self-assembled films do not require annealing to impart insolubility. Significantly, after four-week immersion in DMEM cell culture media,

---

*Corresponding author. Fax: (860)-486-4745; E-mail: papadim@mail.ims.uconn.edu

DOI: 10.1081/MA-120014846
1060-1325 (Print); 1520-5738 (Online)
www.dekker.com

HAs/Fe^{3+} assembled films were devoid of calcium phosphate. Moreover, their hydrolytic stability was found to be dependent on film growth conditions and optimum stability was obtained when the films were assembled at pH and ionic strengths comparable to those of the in vitro testing media.

Key Words: Self-assembly; Semi-permeable membranes; Calcification; Nafion; Humic acids

INTRODUCTION

Among the major impediments hindering the widespread use of implantable biosensors are membrane degradation, calcification, protein fouling as well as inflammation and fibrosis.[1,2] Nafion™ has been frequently used in sensors as a semi-permeable and protective membrane,[3–6] due to its good mechanical and thermal properties,[7] in vivo stability, as well as its chemical and biological inertness.[8,9] Unfortunately, the strong ion-exchange properties of Nafion resulted in significant calcification, in both in vitro and in vivo environments.[10] The fundamental problem lies in the acidic sulfonate groups (R-SO_3H) that decorate the hydrophilic channels in these membranes, acting as sites for nucleation and growth of calcium phosphate crystals, which ultimately inhibit glucose transport and tend to embrittle these Nafion membranes.[10] Moreover, in implantable devices, Nafion has been associated with fibrosis of the surrounding tissue leading to loss of vascularization and restricted analyte flow. The aforementioned drawbacks lead to premature sensor failure.[10]

The motivation for this study was to investigate whether mineralization in thin-film ionic materials like Nafion can be decreased or eliminated by employing layer-by-layer self-assembly processes with strong chelators such as multivalent cations (e.g. Fe^{3+}), a venue that has not been explored before. Nafion, although exhibiting unfavorable tissue reaction upon implantation, was chosen as a model material on account of its wide applicability as membrane material. Initial studies on spin-coated Nafion membranes preincubated with ferric chloride had shown a significant decrease in calcareous deposits.[11] The simplistic approach of electrostatic layer-by-layer assembly of Nafion and ferric ions from dilute solutions should not only allow for a controllable film growth but also for saturation of the sulfonate groups in Nafion with Fe^{3+}. In addition, since Fe^{3+} forms stronger complexes with sulfonate groups, as compared to Ca^{2+}[12] the driving force for calcification was expected to decrease significantly.

The apparent need to replace Nafion with a more bio-acceptable membrane forming material, capable of withstanding the strong in vivo oxidative environment subsequently directed our attention to Humic Acids (HAs), a naturally occurring polyelectrolyte. Humic acids are biopolymers found in soil, sediments, water and some plants like peat and tobacco.[13–16]

HAs are thought to be the final product of the biodegradative and oxidative route, with a mean residence time up to 1200 years in soil.[17] HAs are also very heterogeneous in nature and contain species with molecular weight ranging from a few thousand Daltons to hundreds of kiloDaltons. Their structure is dominated by aromatic building blocks, which are functionalized mostly with carboxy, phenolic, catecholic, quinoid and alcoholic groups, along with few amine groups.[18–20] The variety of functional groups on HAs and their profound electrostatic and chelating abilities allow for interactions with metals,[21] absorption to a variety of surfaces such as minerals,[22–26] cellulose,[27] chitin[28] and bacteria[24] and render them as prime candidates for novel self-assembled membranes.

The present manuscript elaborates on the feasibility of weak and strong polyelectrolytes to assemble with ferric ions and on the effect of experimental parameters on film growth, stability and resistance to mineralization.

EXPERIMENTAL

Materials and Reagents

Nafion™ was obtained from Aldrich as a 5% w/v mixture in water and lower aliphatic alcohols (1100 equivalent weight i.e., 1100 g of polymer per mol of -SO_3H groups). Humic acid, lot # 11909LR, was purchased from Aldrich and was used without any further purification. The HAs sample used in our studies was characterized by elemental and trace metal analysis, as well as molecular weight and functional groups determination. In particular elemental analysis (as supplied by Aldrich Chemical Company, Inc. and verified within 1% by Galbrith Laboratory) for C, N and H indicated: (%): C 43.7, O 41.8, H 4.02, N 0.94, Na 6.2, Ca 0.9, S 0.7, Fe 0.8, Al 0.6, mg 0.2. Trace metal analysis (in PPM) (as supplied by Aldrich Chemical Company) detected: K 535, Si 260, Mn 175, Ti 164, Sr 139, Ba 90, V 10, Zr 9, Cu 6, Li 4, Cr 2. Gel Permeation Chromatography (GPC) in N-methyl pyrolidone/water (9:1) mixture indicated a weight average molecular weight of 169 kDa with polydispersity index $Mw/Mn = 2.58$. Volumetric titration (from pH 2.5 to 12) showed a cumulative acidic functionality content on the order of 820 mequiv/100 g of HAs. The intermediate deflection points in the titration curve ((I) pH 3.2; (II) pH 5.8 and 6.8; (III) pH 10.3) indicated presence of different types of acidic groups ((I) aromatic carboxylic groups ortho to phenolic substitutions; (II) weak aromatic and aliphatic carboxylic acids; (III) phenolic and catecholic-OH).

1 mg/mL HAs solution in deionized water and 1 mg/mL Nafion solution (prepared by diluting the as received solution in a (9:1) methanol/water mixture) were used for all experiments. pH of polyelectrolyte solutions used for the assembly was adjusted with diluted hydrochloric acid (J. T. Baker)

and NH_4OH (Acros); the ionic strength of these solutions were modified by the addition of A.C.S. certified potassium chloride (Fischer). A 5 mg/mL solution of iron(III) chloride hexahydrate ($FeCl_3 \times 6H_2O$) (Aldrich) was used for the self-assembly. Millipore quality deionized water with resistivity >18 MΩ was utilized in all experiments.

The self-assembled films were deposited either on silicon wafers, glass slides or quartz crystal resonators. Silicon wafers and glass slides were cleaned in piranha solution (H_2SO_4/H_2O_2 (7:3)), rinsed with deionized water and methanol, kept in deionized water overnight and used for the self-assembly without further surface modification. 9 MHz AT cut quartz crystal resonators with silver electrode (surface area of 0.32 cm^2; USI, Japan) were used for the QCM experiments. Prior to film deposition, the resonators were immersed for ca. 20 sec in ethanol/water/potassium hydroxide mixture (59/40/1), rinsed in deionized water and used without further surface modification.

Characterization Methods

An HMS™ Series Programmable Slide Stainer from Carl Zeiss, Inc. was used to deposit the self-assembled films. The sample holder was covered to reduce solvent evaporation, thereby improving film quality.

A Hewlett-Packard Network Analyzer (HP-1005A, 10 kHz–300 MHz) was utilized to detect changes in the fundamental frequency after every dip cycle during self-assembly. The Sauerbrey equation[29] was used to quantify the change in frequency with the apparent mass deposited on the resonator (Eq. (1)). The term apparent was used to signify the fact that mass values represent true mass only if the films are rigid and not viscoelastic.[30]

$$\Delta f = -2f_o^2 \Delta m/A\ (\mu_Q \rho_Q)^{0.5} \qquad (1)$$

where: f_o is the resonant frequency of the quartz resonator, Δm is the mass change, A is the active surface area, μ_Q is the shear modulus of quartz, and ρ_Q is the density of quartz.

The thickness of self-assembled films was independently determined by ellipsometry. Ellipsometric data was acquired using a variable angle WVA-SE32™ Spectroscopic Ellipsometer; J. A. Woolman Co., Inc. Films were scanned in the range 250–1000 nm at the incident angles of 65°, 70°, and 75°. Data were collected every 10 nm at 10 revolutions per measurement. A standard Cauchy model was used to fit for thickness and optical constants in the entire optical range.

The stability of self-assembled films was evaluated by depositing them on glass slides and monitoring change in UV absorption as a function of immersion time in 100 mL of deionized water or PBS buffer pH 7.4

(phosphate buffer saline, Sigma Diagnostics) in a thermostated bath at 37°C. UV-Vis scans were performed using Perkin-Elmer Lambda 6 spectrophotometer.

Energy Dispersive X-ray Analysis (EDAX): An EDAX-DX4 unit, equipped with CDU^{TM} LEAP^{TM} detector, operating with an Environmental Scanning Electron Microscope (ESEM) was utilized to determine degree of mineralization via elemental analysis. The working distance (sample distance from the detector), magnification and sample tilt was kept constant for every sample. The substrates: self-assembled films of a comparable thickness and a control, Nafion film coated on a supporting polycarbonate membrane, were immersed in Dulbecco's Modified Eagle's Medium (DMEM) for four weeks. This cell culture medium was previously shown to be a good in vitro model solution to study Nafion calcification.[11]

RESULTS AND DISCUSSION

The technique of electrostatic layer-by-layer self-assembly[31] was employed to deposit films of strong (Nafion) and weak polyacids (Humic acids) with oppositely charged ferric ions. The typical assembly cycle consisted of consecutive dipping in polyelectrolyte and ferric chloride solution followed by an in-between washing step in deionized water. This process is schematically depicted in Fig. 1. The wash step is intended to remove loosely bound surface adhered moieties. A detailed experimental description and discussion on the self-assembly process is provided elsewhere.[32,33]

Nafion is a perfluorinated polyelectrolyte (Fig. 2a) and in a methanol/water solvent mixture attains a micellar conformation with the polar sulfonate groups located on the surface and the hydrophobic fluorocarbon backbone buried inside.[32,34] The driving force for the self-assembly is mostly based on electrostatic interactions between ferric ions and the negatively charged Nafion micelles. These micelles can also interact with the protonated silanol groups (Si-OH) on a substrate due to low pH.[35,36] In the case of humic acids, the functional groups, primarily carboxylic (pK_a 4–5)[37] and phenolic/catecholic (pK_a 8–11)[37] provide active sites (Fig. 2b) for the positively charged ferric ions, which result in electrostatic and complexation driven interactions.[38,39] The excess charge on the trivalent iron ions ensures charge reversal on the adsorbed polyelectrolyte layer rendering it positive and allowing the next layer to assemble. Following the above procedure, the deposition of multi-layered films was investigated as a function of pH and ionic strength of polyelectrolyte solution.

The pH of the Nafion solution was found to have a profound influence on film growth. As illustrated in Fig. 3, a relatively fast growth (ca. 40 nm per dip cycle) was observed at pH 3. At a higher pH (pH 4.5) a significantly lower deposition was observed (ca. 6.7 nm per dip cycle). Because of the strong

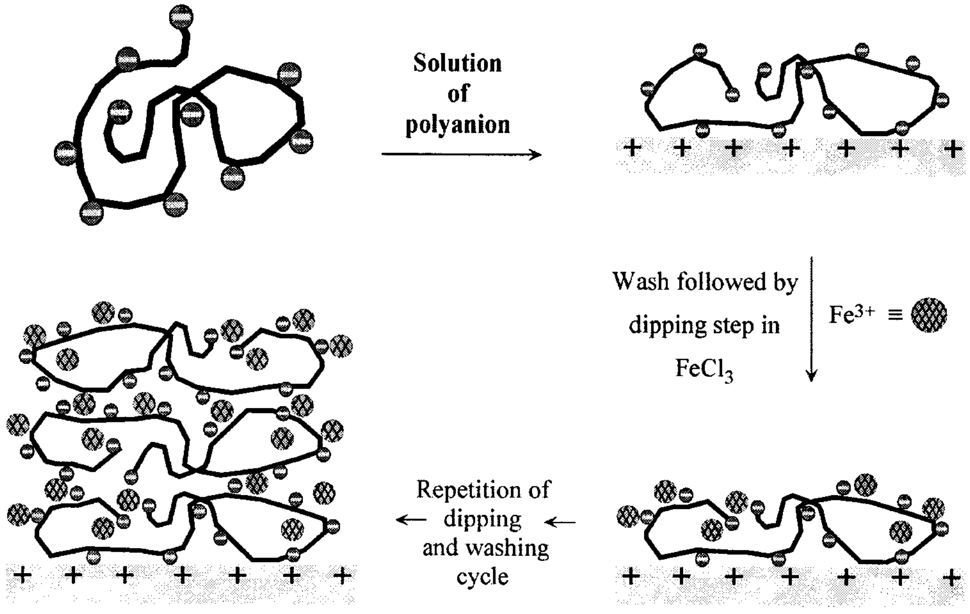

Figure 1. Schematic representation of the layer-by-layer electrostatic/complexation self-assembly process.

acidic character of sulfonate groups in Nafion ($-H_o \sim 12$ on Hammett's scale, comparable with 100% sulfuric acid)[40] a nearly complete ionization is expected for both pH 3 and 4.5. This was also verified by the insensitivity of hydrodynamic radius of Nafion on solution's pH.[32] On the other hand, the formation of insoluble iron hydroxides occurs at pH $\geq$ 4.3 based on the

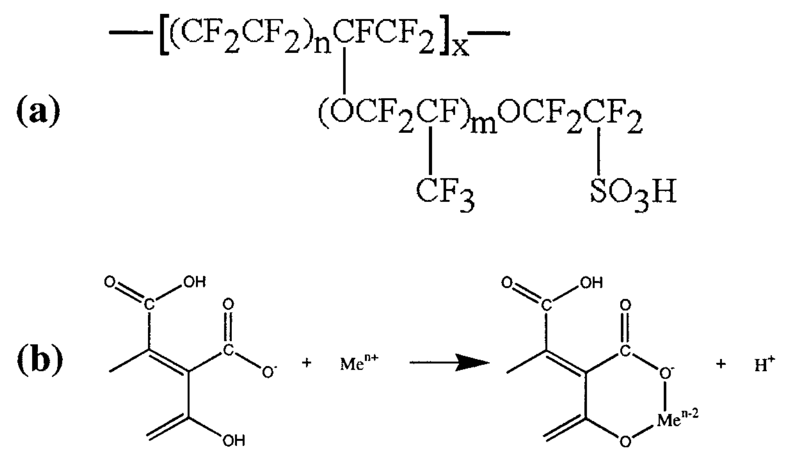

Figure 2. Structural information on the polyelectrolytes used in these assemblies: (a) Nafion, and (b) plausible chelation sites in Humic Acids.

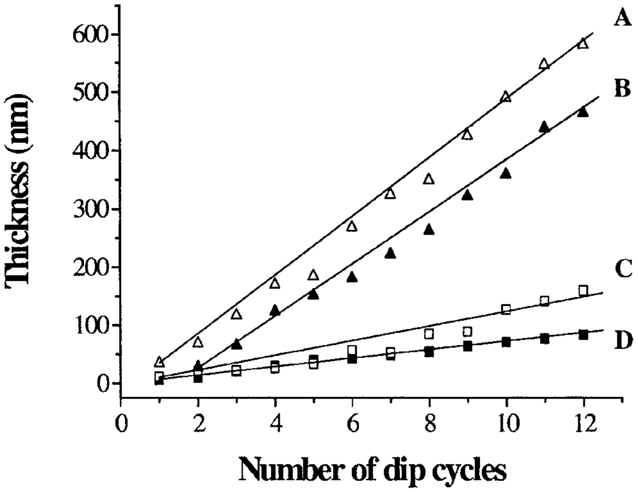

Figure 3. Ellipsometrically determined thickness vs. dip cycle for alternating Nafion/Fe^{3+} assemblies as a function of pH and ionic strength of Nafion solution. (A) pH 3, 0.01 M KCl; (B) pH 3, no salt; (C) pH 4.5, 0.01 M KCl; (D) pH 4.5, no salt. pH of $FeCl_3$ and wash solutions was kept constant at 2 and 7, respectively.

solubility product of $Fe(OH)_3$ ($K_{sp} \sim 6 \times 10^{-39}$).[41] The transformation of adsorbed Fe^{3+} to basic $Fe(RSO_3)_X(OH)_{3-X}$ ($x = 1, 2, 3$; RSO_3 stands for Nafion's ionic groups) results in increase in the basicity of the substrate. Based on these observations, the transition to significantly lower growth rate of the Nafion/Fe^{3+} assemblies above pH 4.5 could be associated with surface induced spreading of Nafion due to acid-base neutralization.

The ionic strength of Nafion solution was also found to have a pronounced effect on film quality and growth. The 0.01 M KCl concentration was determined as optimum ionic strength based on film quality. For 0.1 M KCl or higher, no film deposition was observed and salt was found to preferentially precipitate on the surface. Similarly, screening-reduced adsorption or dehydration of the surface at high ionic strength was observed by other researchers.[42,43] Due to charge screening,[44–49] Nafion, as any other polyelectrolyte, attains a more compact conformation as a result of diminishing repulsive interactions between the negatively charged sulfonate groups. This contributes to a faster growth of 47 nm/dip-cycle (Fig. 3A: pH 3, 0.01 M KCl). Based on our previous dynamic light scattering studies, this growth rate roughly corresponds to the hydrodynamic radius of Nafion in that solution.[32] This indicates that surface adsorption is accompanied with minimum Nafion surface spreading, relative to the salt-free case, where a nearly 65% spreading (with respect to hydrodynamic radius of Nafion in solution) resulted in growth rate of 40 nm/dip-cycle.[32] Thus, at any pH, the resulting growth rate is influenced by the relative strength of the surface-induced interactions that tend to flatten the micelles and the charge-screening forces, which attempt to keep the conformation intact. At pH 4.5 it appears that the basicity of the $Fe(RSO_3)_X(OH)_{3-X}$ surface overpowers the charge-screening forces and causes Nafion spreading.

The optical absorbance of ferric ions provided an additional insight into the film growth and iron incorporation. As shown in Fig. 4 (for pH 4.5 and 0.01 M KCl) the intensity of UV-Vis spectra is gradually increasing as a function of dip cycles. The absorbance at 350 nm (shoulder), associated with iron(III), increases linearly with the number of layers and plotted against the number of dip cycles, follows linear growth pattern (see inset in Fig. 4) similar to that of the ellipsometrically determined thickness shown in Fig. 3. Interestingly, iron concentration, as derived from optical absorbance and film thickness data, was fairly constant throughout the assembly and was independent on the pH and ionic strength and the initially low iron content was associated with various surface effects and inhomogeneities.[33]

Similar to the Nafion system, HAs/Fe^{3+} assembly shows repeatable, stepwise increase in film thickness and deposited mass and the growth rate

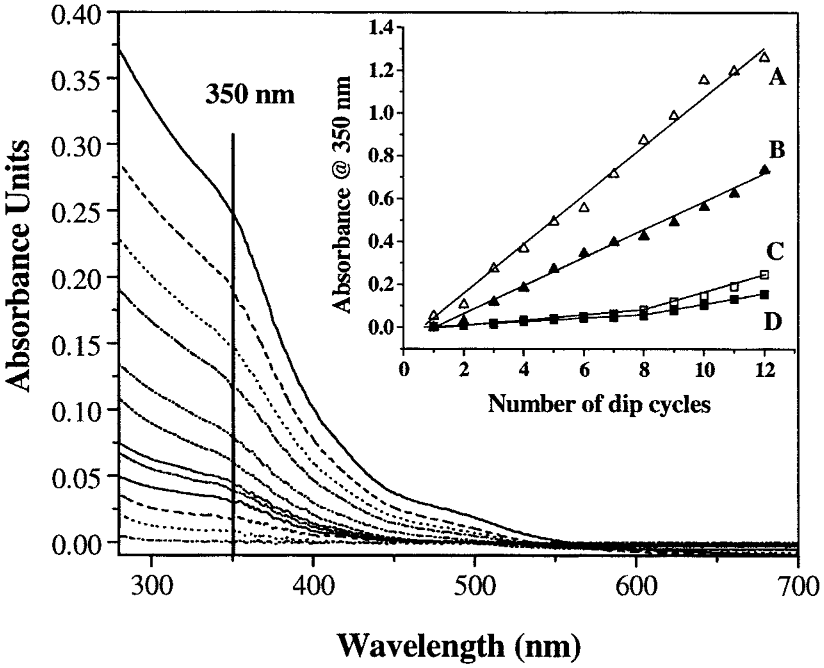

Figure 4. UV-Vis spectra of Nafion/Fe^{3+} assemblies for pH 4.5 and 0.01 M KCl for increasing number of deposited layers. Inset shows the optical absorbance at 350 nm versus number of dip cycles for films deposited at: (A) pH 3, 0.01 M KCl; (B) pH 3, no salt; (C) pH 4.5, 0.01 M KCl; (D) pH 4.5, no salt. The pH of $FeCl_3$ and wash solutions was kept constant at 2 and 7, respectively.

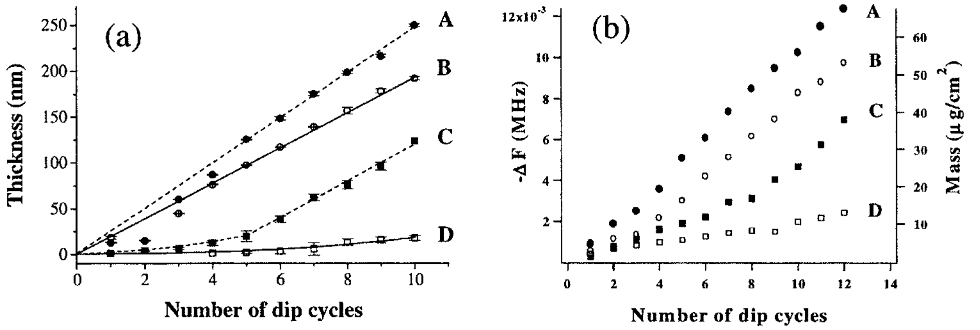

Figure 5. (a) Ellipsometrically determined film thickness and (b) frequency change (left axes) and the calculated mass (right axes) versus dip cycle as a function of pH and ionic strength of HAs solutions for HAs/Fe^{3+} assemblies: (A) pH 5, 0.01 M KCl; (B) pH 5, no salt; (C) pH 9.5, 0.01 M KCl; (D) pH 9.5, no salt.

exhibits strong dependence on pH and ionic strength of the HAs solution, as evidenced by the ellipsometric (Fig. 5 (a) and Table 1) and quartz crystal microbalance (QCM) studies (see Fig. 5 (b) and Table 1). The growth characteristics can be correlated with the conformation of HAs in solution and it's subsequent rearrangement on the surface. The net charge on HAs is governed by the degree of ionization of it's carboxylic and phenolic groups, which in turn is a function of solution pH.[50] At a high pH these weak acidic functionalities are ionized and attain a negative charge resulting in an electrostatic repulsion, both within and between the HA moieties. This allows them to attain an expanded conformation in solution. Iron(III) precipitation in its hydroxide form ($Fe(R)_X(OH)_{3-X}$ (where $x = 1, 2, 3$; and R stands for ionized group on HA) also comes into play at $pH > 4.3$, transforming the iron dominated surface into a strong base and altering the number of

Table 1. A Summary of the Experimentally Determined HAs/Fe^{3+} Film Thickness and Apparent Mass Deposited per Dip Cycle on QCM Resonators as a Function of pH and Ionic Strength of HAs Solution

			Deposited Mass	
pH	KCl [M]	Layer Thickness per Dip Cycle nm	µg*	µg/cm^2
9	—	1.3	0.34	1.06
9	0.01	9.2	0.83	2.59
5	—	19.4	1.34	4.20
5	0.01	24.3	1.80	5.63
3	—	22.1	2.04	6.36

*Mass deposited on QCM resonator in one dip cycle.

available complexation sites.[32] Fewer available sites on iron (III) leads to a lesser degree of charge neutralization on HAs. Moreover, the strong acid-base interactions prevent HAs from attaining globular conformation on the surface and result in surface spreading. Overall the film growth is slower, less than 2 nm per HAs/Fe^{3+} layer at pH = 9.5. At a lower pH the degree of ionization on HA is lesser, leading to enhanced intra- and inter-molecular interaction. This allows the HA molecules to attain a globular conformation and simultaneously aggregate in solution.[51] Upon adsorption on the surface the coiled conformation of the HA molecules is retained because of the hydrophobic interactions, responsible for its globularization, are stronger then the neutralization-induced surface spreading. As a consequence, an increased film deposition is observed with decreasing pH (i.e., 22.1 nm per HA/Fe^{3+} layer at pH 3 (Table 1) vs. 19.4 nm at pH 5). A notable acceleration of film growth is observed on addition of salt (24.3 nm per HA/Fe^{3+} layer at pH 5 and 9.2 nm at pH 9.5). The faster film growth was attributed to salt induced charge screening[52] that leads to more compact HAs conformation capable of further resisting neutralization-induced surface spreading.[32]

The ellipsometric data corroborate well with Quartz Crystal Microbalance (QCM) results, shown in Fig. 5(b). pH and ionic strength dependence appears to follow the pattern seen in ellipsometry. The average mass deposited per dip cycle on the resonator varies from 1.06 μg/cm^2 at pH 9.5 to 6.36 μg/cm^2 at pH 3 in presence of salt (Table 1). This remarkable similarity in film growth on the silicon substrates and on QCM resonators (as well as on glass slides and polymeric supports), suggests that HA/Fe^{3+} self-assembly is substrate independent.

The hydrolytic stability of these self-assembled films is of significance for long-term implantable devices. Figure 6 illustrates the UV-Vis spectra (reflecting Fe^{3+} content) of a 12 layer Nafion/Fe^{3+} film (Nafion pH 3, 0.01 M KCl) immersed in water for 6 weeks. Fourier Transform Infrared (FTIR) spectroscopy suggested that the Nafion to Fe^{3+} ratio remains unchanged throughout the length of this experiment. During the course of one week, only a slight decrease of iron (and subsequently Nafion) was observed, that plateaus thereafter for the duration of the experiment (see inset in Fig. 6a). The initial iron loss (ca. 3.5%, based on integrated intensity) is attributed to loosely attached Nafion moieties, presumably the low molecular weight tail of this polymer.

The stability of the HAs/Fe^{3+} films was strongly interrelated with film growth parameters (i.e., pH and ionic strength) as well as the in vitro media the films were immersed into. Optimum stability was observed for films assembled at pH and ionic strength comparable to the in vitro media. When the stability was tested in PBS buffer, the HAs/Fe^{3+} films deposited from PBS buffer (HAs dissolved in PBS) showed stability similar to Nafion system with only 2–5% iron loss. However, when the pH of the in vitro media was lowered, only insignificant fluctuations in the UV intensity were observed

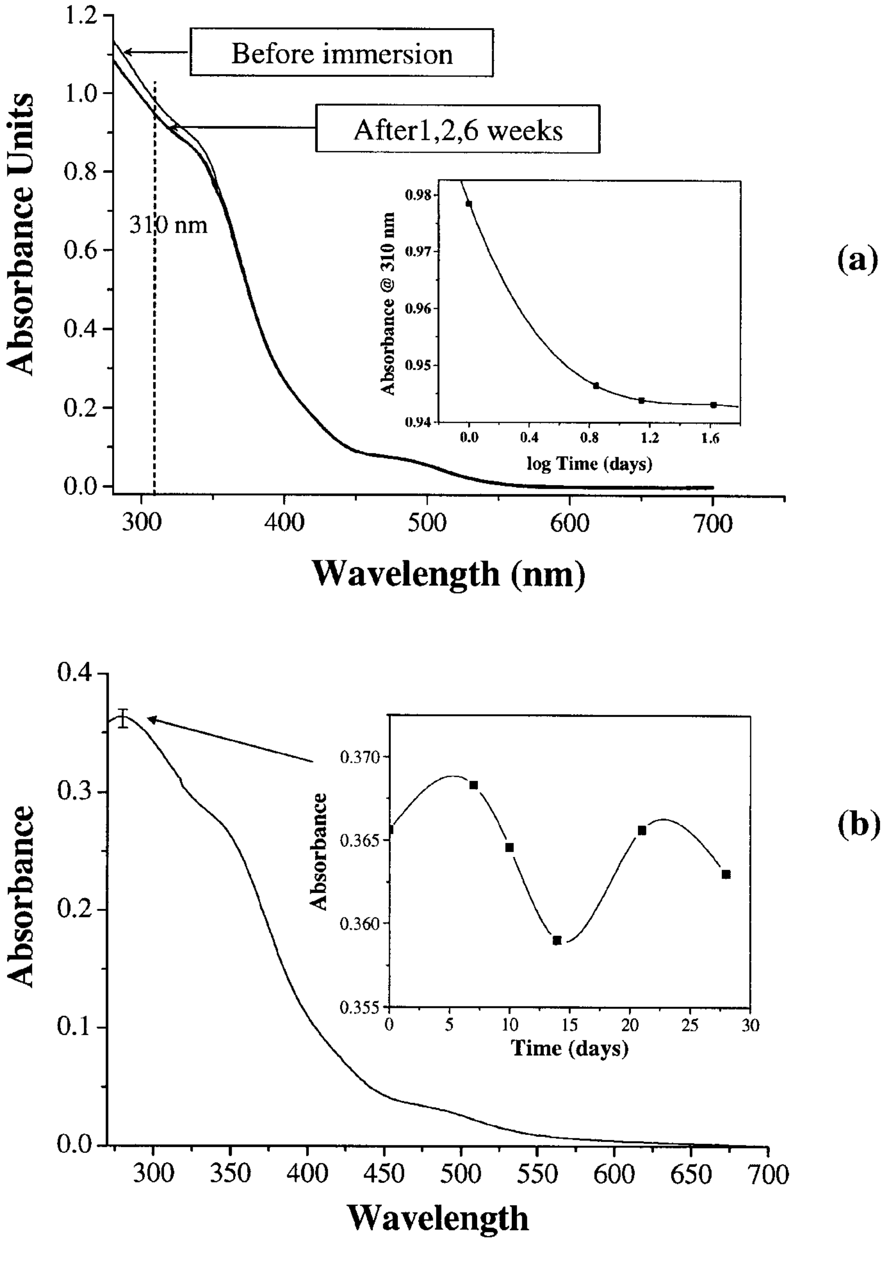

Figure 6. (a) UV-Vis spectra of Nafion/Fe^{3+} film (pH 3, 0.01 M KCl) immersed in water for one to six weeks. The inset shows the absorbance at 310 nm as a function of immersion time; (b) UV-Vis spectra of HAs/Fe^{3+} (PBS buffer, pH 7.4) film immersed in PBS buffer (pH 7.4) for one to four weeks at 37°C.

(see Fig. 6) that can be associated with film quality variations throughout the sample and suggesting that film integrity is somewhat influenced by the pH dependent $Fe^{3+}/Fe(R)_X(OH)_{3-X}$ ratio.

Energy Dispersive X-ray analysis (EDAX) was utilized to investigate the degree of calcification in the self-assembled films (Nafion/Fe^{3+} and HAs/Fe^{3+}) and the results were compared to the spin-coated Nafion films (c.a. 400 nm) after four week immersion in cell culture medium (Dulbecco's Modified Eagle's Medium (DMEM)).[10,11,32] This indicated a more than twenty fold decrease in intensity of adsorbed calcium in the Nafion/Fe^{3+} assemblies as compared to spin-coated and annealed (120°C) Nafion films (Fig. 7). The analysis for the Humic acid system is more complex due to the fact that HAs intrinsically contain both calcium and iron: 0.9 and 0.8 w/w %, respectively (see Experimental section). However, careful comparison of iron to calcium ratio for different areas of the sample indicated that within 5% STD (standard deviation), throughout the duration of the experiment (0–4 weeks), these films were resistance to calcification. This was further supported by the lack of phosphorous line in the spectra. These results suggest that the self-assembly approach may be a viable alternative in reducing calcification of membranes for implantable devices.

As established in our previous studies,[32,33] these self-assembled membranes are semi-permeable to glucose, a very important characteristics pertaining to application in implantable glucose sensors.[10,53] The permeability

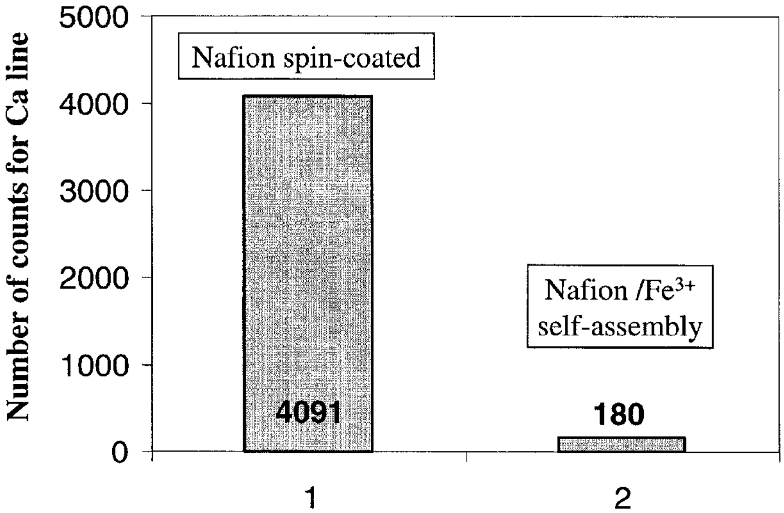

Figure 7. Extent of calcification studied by EDAX. Comparison of calcium line intensity for self-assembled Nafion/Fe^{3+} films and casted Nafion membranes immersed in DMEM nutrient mixture for a period of 4 weeks.

of glucose through the self-assembled films decreases with increasing number of deposited layers. The apparent diffusion coefficient, derived based on our previously reported model[32] for a ca. 400 nm HAs/Fe^{3+} film (twenty dip cycles) on a supporting porous membrane, was on the order of 5×10^{-8} cm^2/sec.[33] This is about two to three orders of magnitude larger than for the Nafion/Fe^{3+} system,[32] suggesting a relatively porous structure for the hydrated HAs/Fe^{3+} membranes.

CONCLUSION

We have described a simple and effective method for fabrication of calcification-resistant semi-permeable membranes intended for implantable sensors and other systems of ionic character as a means of preventing mineralization. Both of the reported systems (i.e., Nafion/Fe^{3+} and HAs/Fe^{3+}) feature controlled film thickness and ability to assemble thick films, with growth rates 47 and 24.3 nm/dip cycle respectively. Along with pH, the charge-screening effects and neutralization induced spreading on the surface comprise the major forces that influence film growth. These self-assembled films exhibited more then an order of magnitude reduction in calcification as compared to the presently used Nafion membranes. Their hydrolytic stability was found to be dependent on film growth conditions with maximum dissolution resistance observed for films assembled at pH and ionic strength comparable to the in vitro testing media. These results, along with the ability to control glucose permeability by varying the number of self-assembled layers, could prove vital in prolonging the lifetime of implantable biosensors.

ACKNOWLEDGMENTS

The authors wish to thank our collaborators: Drs. D. J. Burgess, S. Huang, J. T. Koberstein, D. Kreutzer, and F. Moussy for stimulating discussions. This work was supported by the NIH-R01RR14171, NSF-Career DMR-970220, ONR N00014-00-1-0333 and AFOSR F49620-01-0545 grants.

REFERENCES

1. Gerritsen, M.; Jansen, J.A.; Kros, A.; Nolte, R.J; Lutterman, J.A. Performance of Subcutaneously Implanted Glucose Sensors: A Review. J. Investigative Surgery **1998**, *11*, 163–174.
2. Fraser, D.M. *Biosensors in the Body. Continuous In vivo Monitoring*; Fraser, D. M., Ed.; Wiley: New York, 1998.
3. Hodgson, A.W.E.; Jacquinot, P.; Hauser, P.C. Electrochemical Sensor for the Detection of SO_2 in the Low-ppb Range. Anal. Chem. **1999**, *71*, 2831–2837.

4. Yasuzawa, M.; Matsuki, T.; Mitsui, H.; Kunugi, A.; Nakaya, T. Properties of Glucose Sensors Based on the Immobilization of Glucose Oxidase in Hemocompatible Polypyrrole Film. Chem. Sens. **1998**, *14*, 137–140.
5. Ishiji, T.; Kudo, K.; Kaneko, M. Microenvironmental Studies of an $Ru(bpy)_3^{2+}$ Luminescent Probe Incorporated into Nafion Film and its Application to an Oxygen Sensor. Sensors and Actuators B **1994**, *22*, 205–210.
6. Barton, S.A.C.; Murach, B.L.; Fuller, T.F.; West, A.C. A Methanol Sensor for Portable Direct Methanol Fuel Cells. J. Electrochem. Soc. **1998**, *145*, 3783–3788.
7. Aldrich Technical Bulletin. 1988, 1–5.
8. Wilkins, E.; Atanasov, P.; Muggenburg, B.A. Integrated Implantable Device for Long-Term Glucose Monitoring. Biosens. Bioelect. **1995**, *10*, 485–494.
9. Madaras, M.B.; Buck, R.P. Miniaturized Biosensors Employing Electropolymerized Permiselective Films and their Use for Creating Assays in Human Serum. Anal. Chem. **1996**, *68*, 3832–3839.
10. Mercado, R.C.; Moussy, F. In vitro and In vivo Mineralization of Nafion Membrane Used for Implantable Glucose Sensors. Biosens. Bioelect. **1998**, *13*, 133–145.
11. Valdes, T.I.; Moussy, F. A Ferric Chloride Pre-Treatment to Prevent Calcification of Nafion Membrane Used for Implantable Biosensors. Biosens. Bioelect. **1999**, *14*, 579–585.
12. Sillen, L.G.; Martell, A.E. *Stability Constants of Metal-Ion Complexes*; The Chemical Society: Burlington House, London, 1964.
13. Davies, G.; Radwan, A.; Raffauf, R.F.; Ghabbour, E.A.; Jansen, S.A. Isolation of Humic Acid from the Terrestial Plant. Brugmansia Sanguinea. The Science of the Total Environment **1997**, *201*, 79–87.
14. Ghabbour, E.A.; Khairy, A.H.; Cheney, D.P.; Gross, V.; Davis, G.; Gilbert, T.R.; Zhang, X.J. Isolation of Humic Acid from the Brown Alga *Pilayella littoralis*. J. Appl. Phycol. **1994**, *6*, 459.
15. Willey, R.J.; Davies, G.; Fataftah, A. Supercritical Fluid CO_2 Extraction Accelerates Isolation of Humic Acid from Live *Pilayella littoralis* (Phaeophyta). J. Appl. Phycology **1997**, *8*, 545–551.
16. Radwan, A.; Davies, G.; Fataftah, A.; Ghabbour, E.A.; Jansen, S.A.; Willey, R.J. Isolation of Humic Acid from the Brown Algae *Ascophyllum nodosum, Fucus vesiculosus, Laminaria Saccharina* and the Marine Angiosperm *Zostera Marina*. J. Appl. Phycology **1997**, *8*, 553–562.
17. Stevenson, F.J. In *Humus Chemistry. Genesis, Composition, Reactions*; Stevenson, F.J., Ed.; Wiley & Sons: New York, 1994; 1–23.
18. Stevenson, F.J. In *Humus Chemistry. Genesis, Composition, Reactions*; Stevenson, F.J., Ed.; Wiley & Sons: New York, 1994; 258–263.
19. Paciolla, M.D.; Davis, G.; Jansen, S.A. Generation of Hydroxyl Radicals from Metal-loaded Humic Acids. Environmental Science & Technology **1999**, *33*, 1814–1818.
20. Stevenson, F.J. In *Humus Chemistry. Genesis, Composition, Reactions*; Stevenson, F.J., Ed.; Wiley & Sons: New York, 1994; 221–243.
21. Livens, F.R. Chemical Reactions of Metals with Humic Material. Environmental Pollution **1991**, *70*, 183–208.

22. Vermeer, A.W.P.; Koopal, L.K. Adsorption of Humic Acid to Mineral Particles. 2. Polydispersity Effects with Polyelectrolyte Adsorption. Langmuir **1998**, *14*, 4210–4216.
23. Vermeer, A.W.P.; Riemsdijk, W.H.V.; Koopal, L.K. Adsorption of Humic Acid to Mineral Particles. 1. Specific and Electrostatic Interactions. Langmuir **1998**, *14*, 2810–2819.
24. Fein, J.B.; Boily, J.-F.; Guclu, K.; Kaulbach, E. Experimental Study of Humic Acid Adsorption onto Bacteria and Al-oxide Mineral Surfaces. Chemical Geology **1999**, *162*, 33–45.
25. Schulthess, C.P.; Huang, C.P. Humic and Fulvic Acid Adsorption by Silicon and Aluminum Oxide Surfaces on Clay Minerals. Soil Sci. Soc. Am. J. **1991**, *55*, 34–42.
26. Schlautman, M.A.; Morgan, J.J. Adsorption of Aquatic Humic Substances on Colloidal-Size Aluminum Oxide Particles: Influence o Solution Chemistry. Geochim. Cosmochim. Acta **1994**, *58*, 4293–4303.
27. Jones, K.L.; O'Melia, C.R. Protein and Humic Acid Adsorption onto Hydrophilic Membrane Surfaces: Effects of pH and Ionic Strength. J. Membrane Science **2000**, *165*, 31–46.
28. Ngah, W.S.W.; Musa, A. Adsorption of Humic Acid onto Chitin and Chitosan. J. Applied Polymer Science **1998**, *69*, 2305–2310.
29. Sauerbrey, G.Z. The Use of Quartz Oscillators for Weighing Thin Layers and for Microweighing. Z. Phys. **1957**, *155*, 206–222.
30. Buttry, D.A. In *Electrochemical Interfaces: Modern Techniques for In-situ Interface Characterization*; Abruna, H. D., Ed.; VCH Publishers: New York, 1991; 529–567.
31. Decher, G. Fuzzy Nanoassemblies: Towards Layered Polymeric Multicomposites. Science **1997**, *277*, 1232–1237.
32. Galeska, I.; Chattopadhyay, D.; Moussy, F.; Papadimitrakopoulos, F. Calcification-Resistant Nafion/Fe^{3+} Assemblies for Implantable Biosensors. Biomacromolecules **2000**, *1*, 202–207.
33. Galeska, I.; Hickey, T.; Moussy, F.; Kreutzer, D.; Papadimitrakopoulos, F. Characterization and Biocompatibility Studies of Novel Humic Acid Based Films as Membrane Material for an Implantable Glucose Sensor. Biomacromolecules **2001**, *2*, 1249–1255.
34. Uchida, M.; Aoyama, Y.; Eda, N.; Ochta, A. New Preparation Method for Polymer Electrolyte Fuel Cells. J. Electrochem. Soc. **1995**, *142*, 463.
35. Iler, R.K. Multilayers of Colloidal Particles. J. Colloid Interface Sci. **1996**, *21*, 569–594.
36. Lvov, Y.; Ariga, K.; Onda, M.; Ichinose, I.; Kunitake, T. Alternate Assembly of Ordered Multilayers of SiO_2 and other Nanoparticles and Polyions. Langmuir **1997**, *13*, 6195–6203.
37. March, J. In *Series in Advanced Chemistry: Advanced Organic Chemistry. Reactions, Mechanism, and Structure*; McGraw-Hill, 1977.
38. Schnitzer, M.; Skinner, S.I.M. Organo-Metallic Interactions in Soils: Carboxyl and Hydroxyl Groups in Organic Matter and Metal Retention. Soil Science **1965**, *99*, 278–284.
39. Stevenson, F.J. In *Humus Chemistry. Genesis, Composition, Reactions*; Stevenson, F.J., Ed.; Wiley & Sons: New York, 1994; 348–354.

40. Waller, F.J.; Scoyoc, R.W.V. Chemtech. **1987**, *17*, 438–441.
41. Ebbing, D.D. *General Chemistry*; Houghton Muffin Company, 1996.
42. Clark, S.L.; Montague, M.F.; Hammond, P.T. Ionic Effects of Sodium Chloride on the Templated Deposition of Polyelectrolytes Using Layer-By-Layer Ionic Assembly. Macromolecules **1997**, *30*, 7237–7244.
43. Clark, S.L.; Hammond, P.T. Engineering the Microfabrication of Layer-By-Layer Thin Films. Advanced Materials **1998**, *10*, 1515–1519.
44. Drifford, M.; Dalbiez, J.P. Effect of Salt on Sodium Polystyrene Sulfonate Measured by Light Scattering. Biopolymers **1985**, *24*, 1501–1514.
45. Brender, C. Coil to Rod Transitions in Monte Carlo Simulations of a Short Polyelectrolyte. I. New Thermal and Screening Effects. J. Chem. Phys. **1990**, *92*, 4468–4472.
46. Golestanian, R.; Kardar, M.; Liverpool, T.B. Collapse of Stiff Polyelectrolytes Due to Counterion Fluctuations. Phys. Rev. Lett. **1999**, *82*, 4456–4459.
47. Muthukumar, M. Double Screening in Polyelectrolyte Solutions: Limiting Laws and Crossover Formulas. J. Chem. Phys. **1996**, *105*, 5183–5199.
48. Wolterink, J.K.; Leermakers, F.A.M.; Flee, G.J.; Koopal, L.K.; Zhulina, E.B.; Borisov, E.B. Screening in Solutions of Star-Branched Polyelectrolytes. Macromolecules **1999**, *32*, 2365–2377.
49. Woodward, C.E.; Joensson, B. Monte Carlo and Mean Field Studies of a Polyelectrolyte in Salt Solution. Chem. Phys. **1991**, *155*, 207–219.
50. Swift, R.S. In *Humic Substances II. In Search of Structure*; Hayes, M.H.B., Ed.; Wiley & Sons: New York, 1989; 449.
51. Wershaw, R.L. In *Humic Substances II. In Search of Structure*; Hayes, M.H.B., Ed.; Wiley: New York, 1989; 545.
52. Stevenson, F.J. In *Humus Chemistry. Genesis, Composition, Reactions*; Stevenson, F.J., Ed.; Wiley & Sons: New York, 1994; 285–308.
53. Gerritsen, M.; Jansen, J.A.; Lutterman, J.A. Performance of Subcutaneously Implanted Glucose Sensors for Continuous Monitoring. Neth. J. Med. **1999**, *54*, 167–179.